JOURNAL OF AGRICULTURAL AND FOOD CHEMISTRY

α-Chaconine-reduced Metastasis Involves a PI3K/Akt Signaling Pathway with Downregulation of NF-κB in Human Lung Adenocarcinoma A549 cells

YUAN-WEI SHIH,[†] PIN-SHERN CHEN,[‡] CHENG-HSUN WU,[†,§] YA-FANG JENG,[†] AND CHAU-JONG WANG*,[†]

Institute of Biochemistry and Biotechnology, Chung Shan Medical University, No. 110, Section 1, Chien-kauo N. Road, Taichung 402, Taiwan, Republic of China, Department of Biotechnology, Chia Nan University of Pharmacy & Science, No. 60, Section 1, Erh-Jen Road, Jen-Te, Tainan 717, Taiwan, Republic of China, and Department of Anatomy, China Medical University, No. 91, Hsueh-Shih Road, Taichung 402, Taiwan, Republic of China

α-Chaconine, isolated from *Solanum tuberosum* Linn., is a naturally occurring steroidal glycoalkaloid in potato sprouts. Some reports demonstrated that α-chaconine had various anticarcinogenic properties. The aim of this study is to investigate the inhibitory effect of α-chaconine on lung adenocarcinoma cell metastasis in vitro. We chosed the highly metastatic A549 cells, which were treated with various concentrations of α-chaconine to clarify the potential of inhibiting A549 cells invasion and migration. Data showed that α-chaconine inhibited A549 cell invasion/migration according to wound healing assay and Boyden chamber assay. Our results also showed that α-chaconine could inhibit phosphorylation of c-Jun N-terminal kinase (JNK) and Akt, whereas it did not affected phosphorylation of extracellular signal regulating kinase (ERK) and p38. In addition, α-chaconine significantly decreased the nuclear level of nuclear factor kappa B (NF-κB) and the binding ability of NF-κB. These results suggested that α-chaconine inhibited A549 cell metastasis by a reduction of matrix metalloproteinase-2 (MMP-2) and matrix metalloproteinase-9 (MMP-9) activities involving suppression of phosphoinositide 3-kinase/Akt/NF-κB (PI3K/Akt/NF-κB) signaling pathway. Inhibiting metastasis by α-chaconine might offer a pivotal mechanism for its effective chemotherapeutic action.

KEYWORDS: α-Chaconine; invasion; migration; metastasis; MMP-2; MMP-9; JNK; ERK; p-38; PI3K/Akt; NF-κB

INTRODUCTION

α-Chaconine is the main steroidal glycoalkaloid in potato sprouts, a glycosylated (trisaccharide) derivative of the aglycone solanidine (**Figure 1**). It is produced in bioactive parts of the plant (flowers, young leaves, sprouts, and tubers), and these substances protect the plant against fungi, insect pests, and herbivores (*1*, *2*). In recent studies, α-chaconine has exhibited its antiproliferative and apoptotic effects on the growth of cancer cells originating from human skin (*3*), liver (*4*), prostate, breast, and colon (*5*). In addition to the cytotoxicity in various cancer cells, α-chaconine induces significant cytotoxicity in Chang, normal human liver cells (*6*). However, the precise impact and related molecular mechanism of α-chaconine on metastasis of cancer cells was still unclear.

Lung cancer is the most frequent cause of cancer-related death and accounts for around more than a million deaths yearly worldwide (*7*). Approximately 40% of lung cancers are adenocarcinomas. Adenocarcinomas, which belong to the subgroup of the nonsmall-cell lung cancers are the most common type in the US and Asia, and its frequency is rising in the world (*8*). Studies have shown that lung cancer cases are caused by smoking, air pollution, environmental risk factors (i.e., exposures to radiation, asbestos, heavy mentals, and polycyclic aromatic hydrocarbon), and oncogenes (for example, the Slug gene) (*9*, *10*). Most diagnosed patients with lung adenocarcinoma are in an advanced stage because of its highly metastatic properties, and such patients are not candidates for surgical resection.

The metastasis is a multistep process involving an overexpression of proteolytic enzymes, such as the MMPs family, MMP-2 and MMP-9 (also known as type IV collagenases or gelatinases) which are capable of degrading most ECM components that form the basal membrane (*11*). Therefore, these two gelatinases are essential for tumor cell migration, tumor spreading, tissue invasion of tumor cells, and metastasis (*12*). Gelatinases (MMP-2 and MMP-9) are the major proteases in lung cancer and are closely correlated with invasive and metastatic potentials (*13*).

* Corresponding author. Phone: +886 4 24730022 × 11670, fax: +886 4 23248167, e-mail: wcj@csmu.edu.tw.
[†] Chung Shan Medical University.
[‡] Chia Nan University of Pharmacy and Science.
[§] China Medical University.

10.1021/jf072423r CCC: $37.00 © 2007 American Chemical Society
Published on Web 11/29/2007

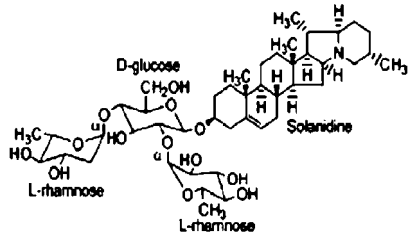

Figure 1. Chemical structure of α-chaconine isolated from the sprouts of potato (*Solanum tuberosum*).

As well as MMPs, the mitogen-activated protein kinases family members (MAPK) are also known to mediate metastasis. The MAPK serine/threonine kinase superfamily is activated by numerous extracellular stimuli and is involved in signal transduction cascades that play an important regulatory role in cell growth, differentiation, apoptosis, and metastasis (*14*). Three major mammalian MAPKs have been described: ERK1/2 or p44/42 MAPK, c-Jun N-terminal kinase/stress-activated protein kinase (JNK/SAPK), and p38 MAPK. The diverse MAPK members are activated in response to different extracellular stimuli and have distinct downstream targets, thus serving different roles in cellular responses. ERK1/2, p38 MAPK, and JNK/SAPK play a central role in regulating the expression of MMPs (*15*). Inhibition of the MAPK pathway might have the potential to prevent angiogenesis, proliferation, invasion, and metastasis for a wide range of tumors. In addition, the PI3K signal transduction pathway regulates cell invasion and metastasis of nonsmall-cell lung cancer (NSCLC) and is closely associated with the development and progress of various tumors. Overexpression of PI3K and low expression of phosphatase and tensin homologue deleted on chromosome 10 (PTEN) are closely correlated with the development, invasion, and metastasis of NSCLC (*16*). Moreover, MMPs gene expression is chiefly regulated by transcriptional factors (for example, NF-κB) via MAPK or PI3K/Akt pathways. NF-κB is a multi-subunit transcription factor involved in cellular responses to viral infection and inflammation. The active NF-κB consists of a dimer of a REL family/p65 subunit and a p50 or p52 subunit. NF-κB is maintained in the cytoplasm through interactions with inhibitors of NF-κB (IκB), but upon dissociation, it moves into the nucleus and promotes cancer cells proliferation, angiogenesis, and metastasis.

This objective of this work was to examine the inhibitory effects and the molecular mechanisms of α-chaconine on the invasion/migration of human lung adenocarcinoma A549 cells in vitro.

MATERIALS AND METHODS

Materials. α-Chaconine, dimethyl sulfoxide (DMSO), Tris-HCl, EDTA, sodium dodecyl sulfate (SDS), phenylmethylsulfonyl fluoride, bovine serum albumin (BSA), leupeptin, Nonidet P-40, deoxycholic acid, and sodium orthovanadate were purchased from Sigma-Aldrich (St. Louis, MO); The protein assay kit was obtained from Bio-Rad Laboratories. (Hercules, CA). Dulbecco's phosphate buffer solution (PBS), trypsin-EDTA, and powdered Dulbecco's modified Eagle's medium (DMEM) were purchased from Gibco/BRL (Gaithersburg, MD). Matrigel was from BD Biosciences (Bedford, MA). Antibodies against Akt, MAPK/ERK1/2, p38 MAPK, and JNK/SAPK, proteins, and phosphorylated proteins were purchased from Cell Signaling Tech. (Beverly, MA). PI3K(p85), NF-κB (p65), and C23 antibodies were from BD Transduction Laboratories (San Diego, CA). β-Actin was from Sigma-Aldrich (St. Louis, MO). The enhanced chemiluminescence (ECL) kit was purchased from Amersham Life Science (Amersham, UK).

Cell Culture and α-Chaconine Treatment. A549, a human lung adenocarcinoma cell line, was obtained from BCRC (Food Industry Research and Development Institute). Cells were cultured in DMEM supplemented with 10% fetal calf serum, 2 mM L-glutamine, 100 U/mL of penicillin, and 100 mg/mL streptomycin mixed antibiotics and 1 mM sodium pyruvate. All cell cultures were maintained at 37 °C in a humidified atmosphere of 5% CO_2−95% air. The culture medium was renewed every 2 to 3 days. Adherent cells were detached by incubation with trypsin (Sigma). For α-chaconine treatment, the stock solution of α-chaconine was dissolved in DMSO and sterilized by filtration through 0.2 μm disk filters. Appropriate amounts of stock solution (1 mg/mL in DMSO) of α-chaconine were added into the cultured medium to achieve the indicated concentrations (final DMSO concentration was less than 0.2%) and then incubated for the indicated time periods.

Analysis of Cell Viability (MTT assay). To evaluate the cytotoxicity of α-chaconine, the MTT [3-(4,5-dimethylthiazol-2-yl)-2,5-diphenyltetrazolium bromide] assay was performed to determine the cell viability (*17*). Briefly, cells were seeded at a density of 4×10^4 cells/well in a 24-well plate for 24 h. Then, the cells were treated with α-chaconine at various concentrations (0, 1, 1.25, 1.5, 1.75, and 2.0 μg/mL) and with 0.2% DMSO as the solvent control for various periods of time (24 and 48 h). Each concentration was repeated three times. After the exposure period, the medium was removed, followed by washing the cells with PBS. Then, the medium was changed and incubated with MTT solution (5 mg/mL)/well for 4 h. The medium was removed, and formazan was solubilized in isopropanol and measured spectrophotometrically at 563 nm. The percentage of viable cells was estimated by comparison with untreated control cells.

Wound Healing Assay. For cell motility determination, A549 cells (1×10^5 cells/well) were plated in 6-well tissue culture plates and were grown to 80–90% confluence. After aspirating the medium, the center of the cell monolayers were scraped with a sterile micropipette tip to create a denuded zone (gap) of constant width. Cellular debris was subsequently washed with PBS, then A549 cells were exposed to various concentrations of α-chaconine (0, 1, 1.25, and 1.5 μg/mL) and 0.2% DMSO as the solvent control. The wound closure was monitored and photographed at 0, 12, 24, 36 and 48 h by an Olympus CK-2 inverted microscope and an Olympus OM-1 camera. To quantify migrated cells, pictures of the initial wounded monolayers were compared with the corresponding pictures of cells at the end of the incubation. Artificial lines fitting the cutting edges were drawn on pictures of the original wounds and overlaid on the pictures of cultures after incubation. Migrated cells across the white lines were counted in six random fields from each triplicate treatment, and data are presented as mean ± standard deviation (SD).

Boyden Chamber Invasion and Migration Assay. The ability of A549 cells to pass through Matrigel-coated filters was measured by the Boyden chamber invasion assay (*18*). Matrigel was diluted to 200 μg/mL with cold filtered distilled water, which was applied to the top side of the 8-μm pore polycarbonate filter. Briefly, A549 cells were treated with various concentrations of α-chaconine. After 48 h, cells were detached by trypsin and resuspended in serum-free medium. Medium containing 10% FBS-medium was applied to the lower chamber as chemoattractant, and then, cells were seeded on the upper chamber at a density of 1.5×10^4 cells/well in 50 μL of serum-free medium. The chamber was incubated for 8 h at 37 °C. At the end of incubation, the cells in the upper surface of the membrane were carefully removed with a cotton swab, and cells that invaded across the Matrigel to the lower surface of the membrane were fixed with methanol and stained with 5% Giemsa solution. The invasive cells on the lower surface of the membrane filter were counted with a light microscope. The data are presented as the average number of cells attached to the bottom surface from randomly chosen fields. Each experiment was carried out in triplicate.

To measure the ability of A549 cells to migrate, cells were seeded into a Boyden chamber with 8 μm pore polycarbonate filters that were not coated with Matrigel. Migration of cells were untreated or treated with various concentrations of α-chaconine. The migration assay was measured as described in the invasion assay.

Analysis of MMP-2/MMP-9 Activity (Gelatin Zymography). The activities of MMP-2 and MMP-9 were assayed by gelatin zymography as described previously (*19*). Briefly, conditioned media from cells cultured in the absence of serum for 24 and 48 h were collected.

Samples were mixed with loading buffer. The samples were not boiled before loading and were electrophoresed on 8% SDS-polyacrylamide gel containing 0.1% gelatin. Electrophoresis was performed at 140 and 110 V for 3 h. Gels were then washed twice in zymography washing buffer (2.5% Triton X-100 in double-distilled H_2O) at room temperature to remove SDS, followed by incubation at 37 °C for 12–16 h in zymography reaction buffer (40 mM Tris-HCl (pH 8.0), 10 mM $CaCl_2$, 0.02% NaN_3), and, finally, stained with Coomassie blue R-250 (0.125% Comassie blue R-250, 0.1% amino black, 50% methanol, 10% acetic acid) for 1 h and destained with destaining solution (20% methanol, 10% acetic acid, 70% dd H_2O). Nonstaining bands representing the levels of the latent forms of MMP-2 and MMP-9 were quantified by densitometer measurement using a digital imaging analysis system.

Preparation of Whole-Cell Lysates and Nuclear Extracts. A549 cells (1×10^5 cells) were plated in a 25 cm^2 tissue culture flask and were treated with various concentrations of α-chaconine and 0.2% DMSO. A549 cells were washed twice with PBS and were scraped into a microcentrifuge tube. The cells were centrifuged at 1250*g* for 5 min, and the pellet was lysed with iced-cold RIPA buffer (1% NP-40, 50 mM Tris-base, 0.1% SDS, 0.5% deoxycholic acid, 150 mM NaCl, pH 7.5), to which was added freshly prepared phenylmethylsulfonyl fluoride (10 mg/mL), leupeptin (17 mg/mL), and sodium orthovanadate (10 mg/mL). After incubation for 5 min on ice, the samples were centrifuged at 10000*g* for 10 min, and then the supernatants were collected as whole-cell lysates. The lysates were denatured and subjected to SDS-PAGE and Western blotting. Nuclear extracts were prepared as previously described (*20*) and then used for NF-κB detection. Nuclear pellets were resuspended in nuclear extract buffer (1.5 mM $MgCl_2$, 10 mM HEPES, pH 7.9, 0.1 mM EDTA, 0.5 mM dithiothreitol, 0.5 mM phenylmethylsulfonyl fluoride, 25% glycerol, and 420 mM NaCl). The nuclear suspension was incubated on ice for 20 min and then centrifuged at 14 000*g* for 5 min. The supernatant (corresponding to the soluble nuclear fraction) was saved, and the remaining pellet was solubilized by sonication in PBS. The protein content was determined with Bio-Rad protein assay reagent using BSA as a standard.

Western Blotting Analysis. Whole-cell lysates and nuclear proteins were isolated as described above. To analyze the expression of proteins, cells were grown in 100 mm dishes, cultured, and treated as described in Cell Culture and α-Chaconine Treatment. Western blotting was performed as follows. Whole-cell lysates or nuclear proteins (50 μg of purified protein) were mixed with an equal volume of electrophoresis sample buffer, and the mixture was then boiled for 10 min. Then, an equal protein content of total cell lysate from control, 0.2% DMSO, and α-chaconine-treated sample were resolved on 10–12% SDS-PAGE gels. Proteins were then transferred onto nitrocellulose membranes (Millipore, Bedford, MA) by electroblotting using an electroblotting apparatus (Bio-Rad). Nonspecific binding of the membranes was blocked with Tris-buffered saline (TBS) containing 1% (w/v) nonfat dry milk and 0.1% (v/v) Tween-20 (TBST) for more than 2 h. Membranes were washed with TBST three times for 10 min and then incubated with an appropriate dilution of specific primary antibodies in TBST overnight at 4 °C. The membranes were wubsequently washed with TBST and ithen ncubated with an appropriate secondary antibody (horseradish peroxidase-conjugated, goat antimouse, or antirabbit IgG) for 1 h. After washing the membrane three times for 10 min in TBST, the bands were revealed by enhanced chemiluminescence using ECL Western blotting detection reagents and exposed ECL hyperfilm in a FUJIUM Las-3000. Then proteins were quantitatively determined by densitometry using FUJIFILM-Multi Gauge V2.2 software.

Electrophoretic Mobility Shift Assay (EMSA) of Nuclear NF-κB. Cell nuclear proteins were extracted by nuclear extract buffer and then measured by electrophoretic mobility shift assay (EMSA) (*21*). Cells (1×10^5) were collected in PBS buffer (pH 7.4) and were centrifuged at 2000*g* for 5 min at 4 °C. Cells were lysed with buffer A (10 mM HEPES, 1.5 mM $MgCl_2$, 10 mM KCl, 0.5 mM DTT, and 0.5 mM PMSF (pH 7.9) containing 5% NP-40) for 10 min on ice, and this was followed by vortexing to shear the cytoplasmic membranes. The lysates were centrifuge at 2000*g* for 10 min at 4 °C. The pellet containing the nuclei was extracted with high-salt buffer C (20 mM HEPES, 420 mM NaCl, 1.5 mM $MgCl_2$, 0.5 mM DTT, 0.5 mM PMSF, 0.2 mM EDTA, and 25% glycerol) for 15 min on ice. The lysates were clarified by centrifugation at 13 000*g* for 10 min at 4 °C. The supernatant containing the nuclear proteins was collected and frozen at −80 °C until use. The protein content of nuclear fractions was determined with the Bio-Rad protein assay. A 5 μg aliquot of nuclear proteins was mixed either with biotin-labeled NF-κB oligonucleotide probes for 15 min at room temperature or with oligonucleotides containing (sense of NF-κB, 5′-AGTTGAGGGGACTTTCCCAG GC-3′, antisense of NF-κB, 3′-TCAACTCCCCTGAAAGGGTCCG-5′). DNA probes were added to 20 μL of binding reactions containing double-distille H_2O, 5 μg of nuclear protein, 1 μL of poly L-lysine, 1 μL of poly (dI-dC), 2 μL of biotin-labeled double-stranded NF-κB oligonucleotides, and 2 μL of 10-fold binding buffer in a microcentrifuge tube, and the mixture was incubated for 15 min at room temperature. Specific competition binding assays were performed by adding a 200-fold excess of unlabeled probe as a specific competitor. Following protein-DNA complex formation, samples were loaded on a 10% nondenaturing polyacrylamide gel in 0.5 × TBE buffer, transferred to positively charged nitrocellulose membranes by a transfer blotting apparatus, and then cross-linked in a Stratagene cross-linker. Gel shifts were visualized with streptavidin-horseradish peroxidase followed by chemiluminescent detection.

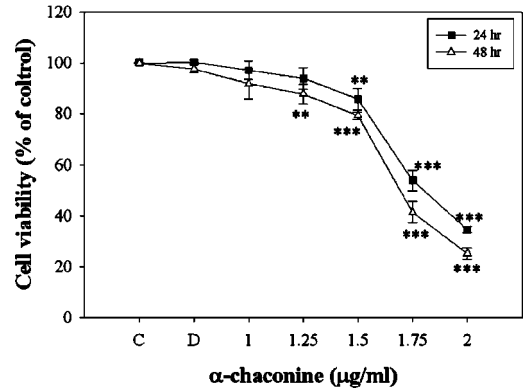

Figure 2. Effect of α-chaconine on the viability of A549 cells. A549 cells (4×10^4 cells/well) were treated with or without α-chaconine, Control (C); 0.2% DMSO (D); 1, 1.25, 1.5, 1.75, and 2 μg/mL; for 24 and 48 h. Cell viability was determined by the MTT assay. Values are expressed as mean ± SD of three independent experiments. $^{**}p < 0.01$, $^{***}p < 0.001$ compared with the untreated control. 0.2% DMSO is the solvent control.

Statistical Analysis. Data were expressed as means ± SD of three independent experiments and were analyzed by Student's *t*-test (Sigmaplot 2001). Significant differences were established at $P \leq 0.05$.

RESULTS AND DISCUSSION

Chemical Structure of α-Chaconine. Potato glycoalkaloids (GAs), mainly α-chaconine and α-solanine, comprise 95% of all GAs (*22*). **Figure 1** shows that α-chaconine is constructed of a branched β-chacotriose (bis-α-L-rhamnopyranosyl-β-D-gluco-pyranose) carbohydrate side chain attached to the 3-OH group of the aglycon solanidine.

Cytotoxicity of α-Chaconine in A549 Cells. We first assayed the cytotoxicity of α-chaconine on the lung adenocarcinoma cell line, A549. As shown in **Figure 2**, the level of the cell viability effect of α-chaconine was assayed in a dose- and time-dependent manner, followed by the MTT assay. Compared to the untreated control (0.2% DMSO alone), after 24 and 48 h, treatment with α-chaconine at a concentration between 0 and 1.5 μg/mL was not significantly changed, indicating that α-chaconine was not toxic to A549 cells at these dosages. When cells were treated with 1.75 and 2 μg/mL α-chaconine for 24 and 48 h, cell viability was significantly decreased. These results demonstrated that the treatment of α-chaconine with doses

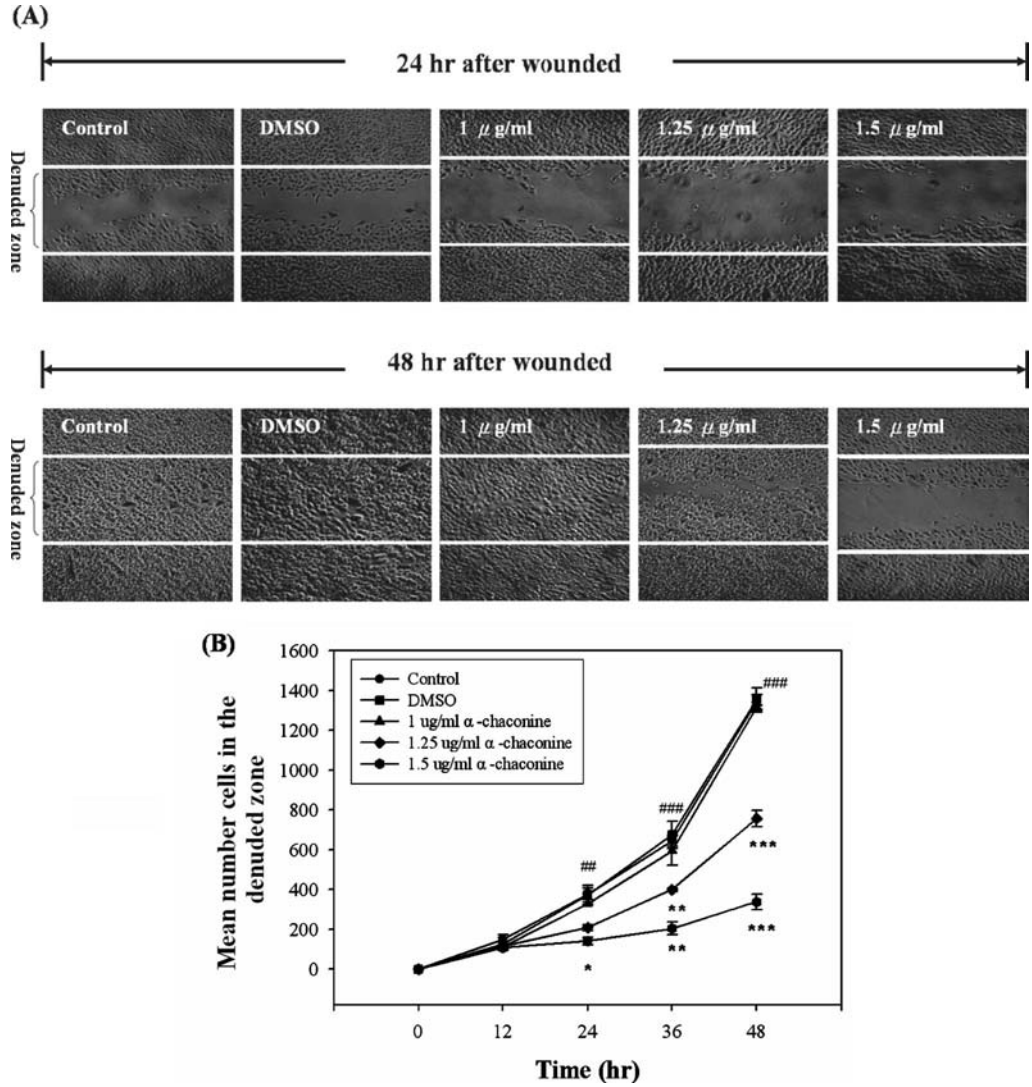

Figure 3. The effect of α-chaconine on the motility of A549 cells. (**A**) A549 cell monolayers were scraped by a sterile micropipette tip, and the cells were treated with or without α-chaconine; Control (C); 0.2% DMSO (D); 1, 1.25, and 1.5 μg/mL for 0, 12, 24, 36, and 48 h. The number of cells in the denuded zone was quantitated after indicated times (0, 12, 24, 36, and 48 h) by inverted microscopy. White lines indicate the wound edge. Only pictures at 24 and 48 h are presented. (**B**) Migrated cells across the white lines were counted in six random fields from each treatment. Quantitative assessment of the mean number cells in the denuded zone are expressed as mean ± SD of three independent experiments. $^{*}p < 0.05$, $^{**}p < 0.01$, $^{***}p < 0.001$ compared with the untreated control; $\#\#p < 0.01$, $\#\#p < 0.001$ compared with the 0 h-treated time".

higher than 1.5 μg/mL for 24 and 48 h resulted in dose- and time- dependent loss of cell viability in A549 cells, but doses lower than 1.5 μg/mL for 24 and 48 h did not cause cytotoxicity. In the following experiments, these doses below 1.5 μg/mL of α-chaconine were used.

α-Chaconine Inhibits the Migration and Invasion of A549 Cells. To investigate the inhibitory effect of α-chaconine on A549 cell migration and invasion process, the wound healing assay and the Boyden chamber assay were used. In the wound healing assay, the confluent monolayer was scraped with a sterile micropipette tip to create a scratch wound. After incubation with 1.25 and 1.5 μg/mL of α-chaconine for 24 and 48 h, the cells migrated to the denuded zone, and they were counted. The results demonstrated that α-chaconine dose-dependently suppressed A549 cell migration to the denuded zone (**Figure 3A**). Treatment with 1.25 and 1.5 μg/mL of α-chaconine inhibited 45 and 63% of cell migration after 24 h, respectively; and such doses of α-chaconine inhibited 50 and 75% of cell migration at 48 h, respectively. Additionally, according to a quantitative assessment, the cells were treated with various concentrations of α-chaconine for 0, 12, 24, 36, and 48 h. The results showed that 1.5 μg/mL of α-chaconine exhibited the most inhibitory effect on cell migration after 48 h incubation (**Figure 3B**). These results revealed that α-chaconine significantly inhibited the motility of A549 cells.

One important characteristic of metastasis is the migratory and invasive ability of tumor cells. We used the Boyden chamber assay to quantify the migratory and invasive potential of A549 cells. The results showed that α-chaconine induced a dose-dependent decrease in migration with increasing concentration of α-chaconine (**Figure 4A**). At 1.25 μg/mL the migration was reduced to 80%, and at 1.5 μg/mL the migration was reduced to less than 50%. Subsequently, α-chaconine also induced a dose-dependent decrease in invasion with increasing concentration of α-chaconine (**Figure 4B**). At 1.25 μg/mL the invasion was reduced to 75%, and at 1.5 μg/mL the invasion was reduced to less than 50%. The results demonstrated that α-chaconine significantly inhibited the migration and invasion of A549 cells.

α-Chaconine Inhibits the Activation of MMP-2 and MMP-9 in A549 Cells. In many types of neoplasm, including lung cancer, higher levels of activated MMPs have been

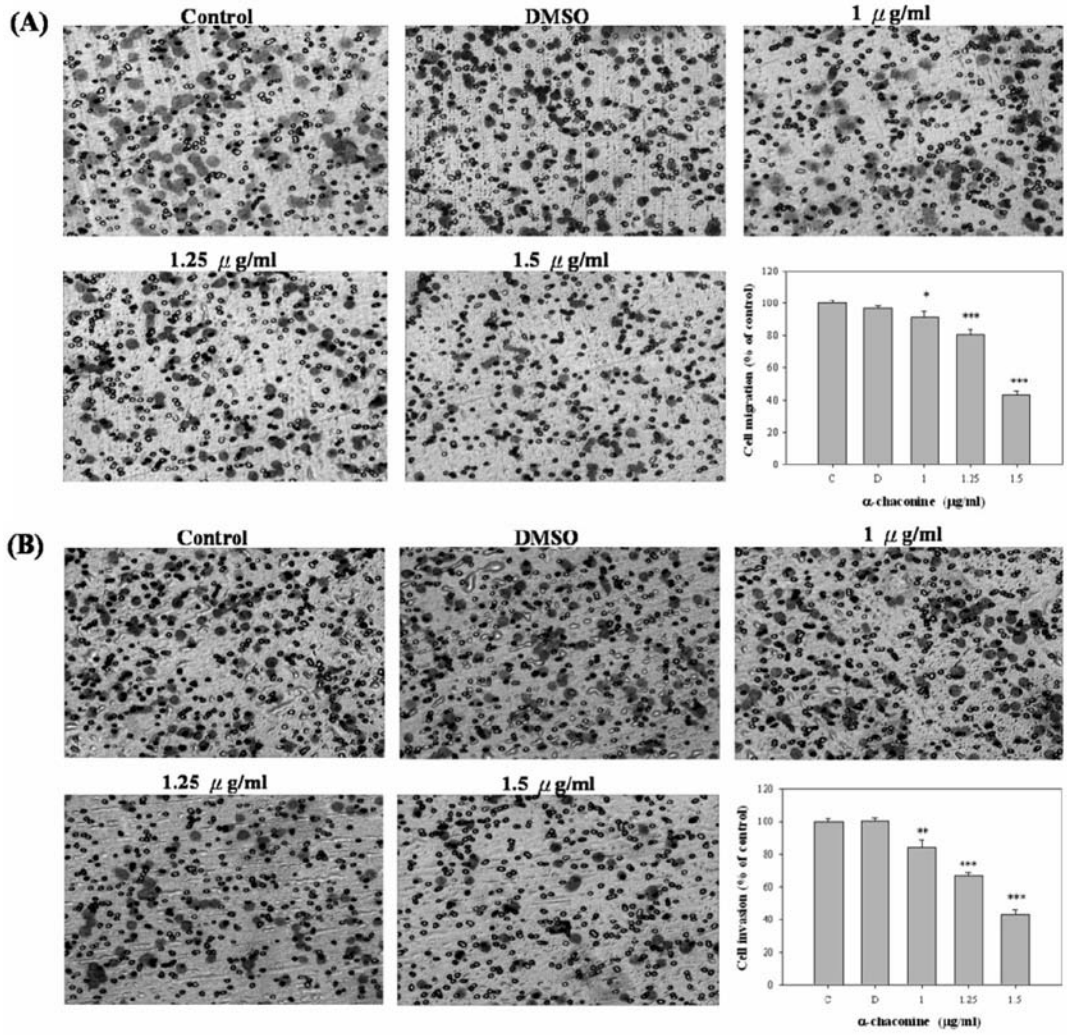

Figure 4. Effect of α-chaconine on migration and invasion of A549 cells. A549 cells were treated with or without α-chaconine; Control (C); 0.2% DMSO (D); 1, 1.25, and 1.5 μg/mL for 48 h. (**A**) Cell migration was measured by Boyden chamber for 6 h with polycarbonate filters (8 μm pore size); (**B**) Cell invasion was measured by Boyden chamber for 8 h; polycarbonate filters (8 μm pore size) were precoated with matrigel. Migration and invasion ability of A549 cells were quantified by counting the number of cells that invaded to the underside of the porous polycarbonate membrane under microscopy, and the results represent the average of three experiments ± SD $*p < 0.05$, $**p < 0.01$, $***p < 0.001$ compared with the untreated control.

demonstrated in more invasive and/or metastatic tumors and may give prognostic information independent of stage (*23*, *24*). Thus, tumor metastasis is highly related to the proteolytic degradation of the extracellular matrix (ECM). To further investigate that matrix-degrading proteinases are required. A549 cells were treated with various concentrations of α-chaconine for 24 and 48 h in serum-free media. At the end of the incubation, media were collected and were assayed for MMPs activity (gelatin zymography), as described in the Materials and Methods section. **Figure 5A** showed that MMP-2 and MMP-9 activities were markedly reduced at 1.5 μg/mL of α-chaconine for 24 h.

Figure 5B demonstrated the effect of α-chaconine treatment for 48 h on the activities of MMP-2 and MMP-9. The results showed that MMP-2 activity was significantly reduced at 1.25 and 1.5 μg/mL of α-chaconine. MMP-9 activity was reduced at 1.5 μg/mL of α-chaconine. The results suggested that the inhibition of MMP-2 by α-chaconine might be more sensitive than MMP-9, and that α-chaconine targets MMP-mediated cellular events in A549 cells and contributes a new mechanism for its anticancer activity.

Malignant tumors invade normal tissue, which involves three independent processes: the degradation of the extracellular matrix (ECM), cell metastasis, and proliferation. Metastasis has been found to be accompanied by various physiological alterations involved in the degradation of ECM, such as the overexpression of proteolytic enzyme activity, such as matrix metaloproteinases (for example, MMP-2 and MMP-9), as well as the invasion of tumor cells into the bloodstream or lymphatic system to spread to another tissue or organ (*25*, *26*). Thus, MMPs play key roles in facilitating the metastasis of tumor cells. Furthermore, the results of the wound healing assay (**Figure 3**, panels **A** and **B**) and the Boyden chamber assay (**Figure 4**, panels **A** and **B**) demonstated that α-chaconine showed significant inhibitory effect on invasion and migration of A549 cells. MMP-2 and MMP-9 expressions have been linked to various cellular and physiological processes, such as cell motility, adhesion, proliferation, activation, differentiation, development, invasion, metastasis, and wound healing, most of which are also known to be modulated by MMPs. Zymographic analysis (**Figure 5**, panels **A** and **B**) showed that treatment with α-chaconine at a subcytotoxic concentration of 1.5 μg/mL for 24 and 48 h exerts an inhibitory effect of MMP-2 and MMP-9. Therefore, α-chaconine was able to inhibit the gelatinolysis of A549 cells mediated by MMP-2 and MMP-9 in a conditioned medium. These results suggested that the

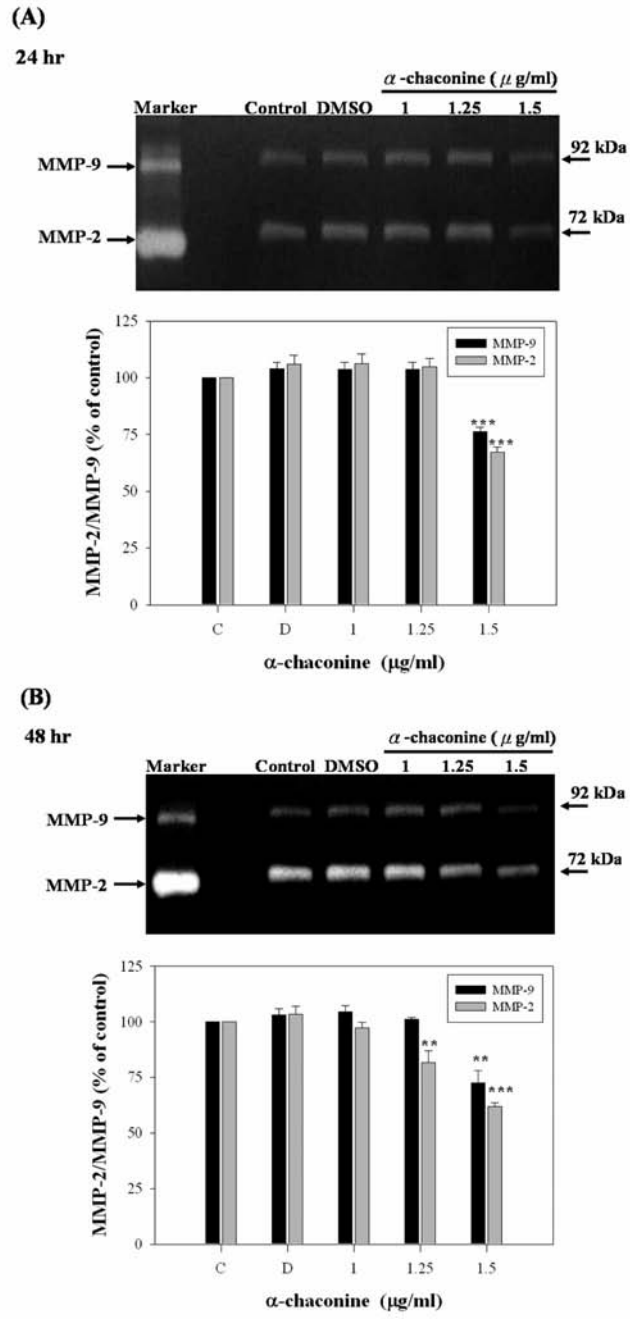

Figure 5. Effect of α-chaconine on MMP-2/MMP-9 activity of A549 cells. Cells were treated with or without α-chaconine; Control (C); 0.2% DMSO (D); 1, 1.25, and 1.5 μg/mL for 24 and 48 h. The conditioned media were collected, and MMP-2/MMP-9 activities were determined by gelatin zymography. MMP-2/MMP-9 activities were quantified by densitomeric analysis. The densitomeric data were expressed as mean ± SD of three independent experiments. $^{**}p < 0.01$, $^{***}p < 0.001$ compared with the untreated control.

anti-invasion effect of α-chaconine was associated with the inhibition of enzymatically degradative processes of tumor metastasis. This was the first report to demonstrate the biochemical mechanism(s) by which α-chaconine reduced the metastasis in human lung adenocarcinoma cells. The expression of MMP-2 and MMP-9 have been shown to play a critical role in degrading the basement membrane in cancer invasion and migration.

α-Chaconine Inhibits Phosphorylation of JNK and Akt. Several studies have indicated that transcription factors NF-kB, JNK1/2, ERK1/2, p38 MAPK, and Akt are involved in activities of MMP-2 and MMP-9 on different cell types (*27, 28*). To assess whether α-chaconine mediates and/or inhibits phosphorylation of JNK1/2, ERK1/2, p38 MAPK, Akt, and the protein level of PI3K, we investigated the effect of α-chaconine on the phosphorylated status of MAPK family members (JNK1/2, ERK1/2, and p38 MAPK) and Akt in A549 cells that were treated with various concentrations of α-chaconine for 3 h and 1.5 μg/mL of α-chaconine for various periods of time (0, 1, 2, 3, and 6 h). **Figure 6A** and **Figure 6B** showed that α-chaconine significantly suppressed the activation of JNK1 and JNK2, as shown by decreasing the phosphorylation of JNK1 and JNK2. In contrast, α-chaconine did not significantly affect phospho-ERK1/2 and phospho-p38 activities (**Figure 6C−F**). In addition, α-chaconine inhibited the protein level of PI3K and phosphorylation of Akt in a dose- and time-dependent manner (**Figure 7**). Data revealed that the activation of PI3K/Akt signaling was related to cancer invasion and metastasis, except MAPK signalings, which mediate human tumor progression (*29*). Data findings revealed that the treatment of α-chaconine diminished the activities of MMP-2 and MMP-9 in the culture media and could possibly involve a suppression of phosphorylation of JNK1/2 and Akt. Here, it was illustrated that α-chaconine decreased the activities of MMP-2 and MMP-9, involving inactivation of PI3K-Akt or JNK1/2 signaling pathways, and that such an inhibitory effect on proteinase expression may contribute to the ability of α-chaconine to inhibit cell invasion and migration.

α-Chaconine Decreases the Nuclear Content of NF-κB and Inhibits DNA Binding Activity of NF-κB in A549 Cells. NF-κB transcriptional factor has been known to translocate to the nucleus and to regulate the expression of multiple genes involved in MMPs secretion. To further explore the activity of NF-κB, the amount of NF-κB in the cell nuclear extracts were measured by Western blotting to analyze the possible inhibitory effect of α-chaconine on the activity of NF-κB. As explained in **Figure 8A**, α-chaconine-treated A549 cells demonstrated a decrease in the protein level of NF-κB. Furthermore, the effect of α-chaconine on the DNA binding activity of NF-κB in A549 cells was investigated by EMSA. As shown in **Figure 8B**, α-chaconine significantly inhibited NF-κB binding activity at 1.5 μg/mL of α-chaconine.

Because several reports have demonstrated that invasion and migration were induced through the activation of JNK, PI3K/Akt, and NF-κB, which seemed to play a central role in regulating the expression of MMP-2 and MMP-9 (*30, 31*). In the present study we demonstrated that α-chaconine could inhibit MMP-2 and MMP-9 activities through inhibiting the binding activity of NF-κB (**Figure 8B**) but not AP-1 (data not shown). Activation of NF-κB, in the PI3K/Akt/NF-κB signaling pathway, has also frequently been reported to play an important role in those pathological processes, such as inflammation, cancer adhesion, invasion, metastasis, and angiogenesis. The effect of α-chaconine on the protein level of NF-κB in nuclear extracts was analyzed by Western blotting, and we have found that the treatment of A549 cells with α-chaconine resulted in a decrease of the NF-κB protein in the nucleus (**Figure 8A**). This is the first report to provide evidence that α-chaconine plays an inhibitory role in phosporylation of JNK and Akt. The results imply that α-chaconine may inhibit the PI3K/Akt/NF-κB signaling pathway and may down-regulate the activities of MMP-2 and MMP-9, by which α-chaconine reduces the metastasis in A549 cells. α-Chaconine markedly decreased the level of phosphorylated JNK (**Figure 6**, panels **A** and **B**), whereas it has been shown that the binding activity of the

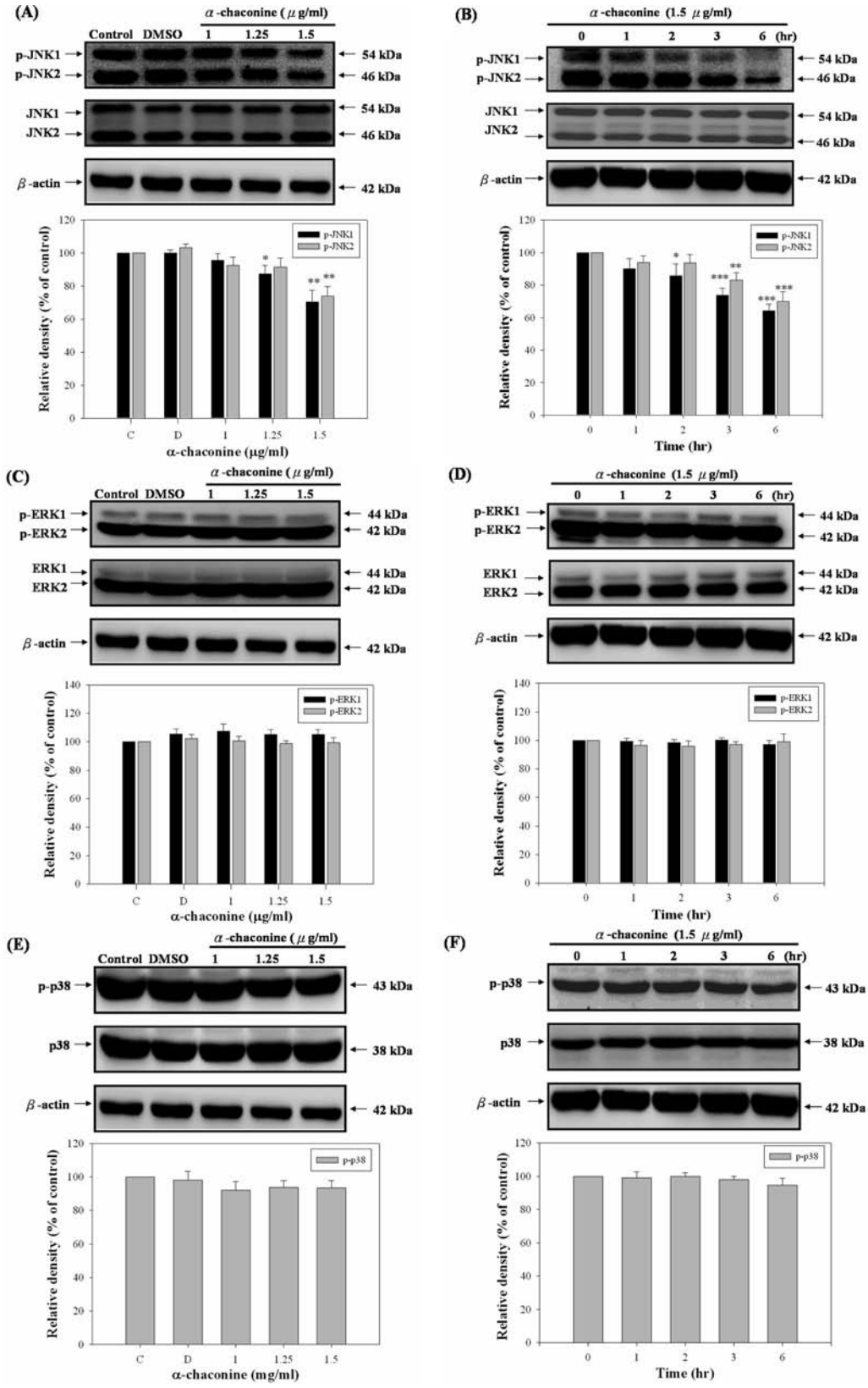

Figure 6. Dose- and time-dependent effect of α-chaconine on the phosphorylation of JNK, ERK, and p38. In the dose-dependent assay (panels **A**, **C**, and **E**), A549 cells were treated with or without α-chaconine; Control (C); 0.2% DMSO (D); 1, 1.25, and 1.5 μg/mL for 3 h. In the time-dependent assay (panels **B**, **D**, and **F**), A549 cells were treated with 1.5 μg/mL of α-chaconine for 0, 1, 2, 3, and 6 h. Activities of JNK phosphorylation, JNK, ERK phosphorylation, ERK, p38 phosphorylation, and p38 were analyzed by Western blotting. β-Actin was used as a loading control. The relative density of phosphorylated forms of JNK, ERK, and p38 were normalized to total values of JNK, ERK, and p38, which were determined by densitometric analysis. Values are expressed as mean ± SD of three independent experiments. $*p < 0.05$, $**p < 0.01$, $***p < 0.001$ compared with the untreated control.

transcription factor AP-1 is unaffected (data not shown). This means that α-chaconine inhibited MMP-2 and MMP-9 activities may be involved in inhibiting the binding activity of NF-κB but not AP-1.

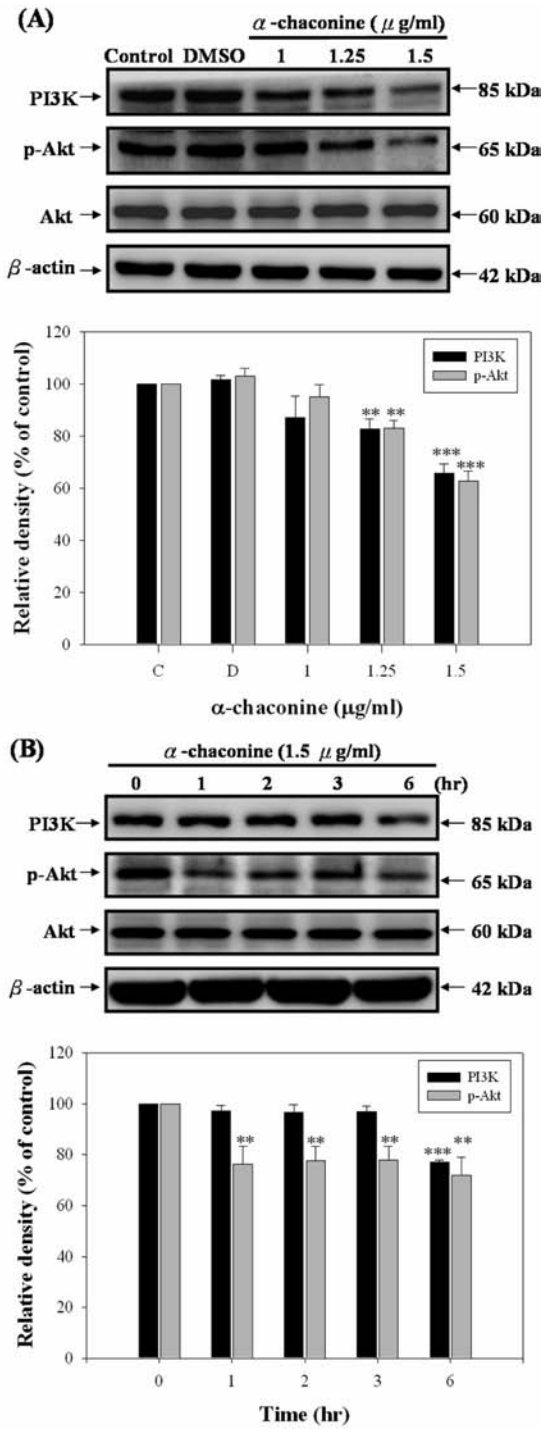

Figure 7. Dose- and time-dependent effects of α-chaconine on the protein expression level of PI3K and on the phosphorylation of Akt. In the dose-dependent assay (**A**) A549 cells were treated with or without α-chaconine; Control (C); 0.2% DMSO (D); 1, 1.25, and 1.5 μg/mL for 3 h. In the time-dependent assay (**B**) A549 cells were treated with 1.5 μg/mL of α-chaconine for 0, 1, 2, 3, and 6 h. The expression of PI3K and phosphorylation of Akt were analyzed by Western blotting. β-Actin was used as a loading control. Values are expressed as mean ± SD of three independent experiments. $^{**}p < 0.01$, $^{***}p < 0.001$ compared with the untreated control.

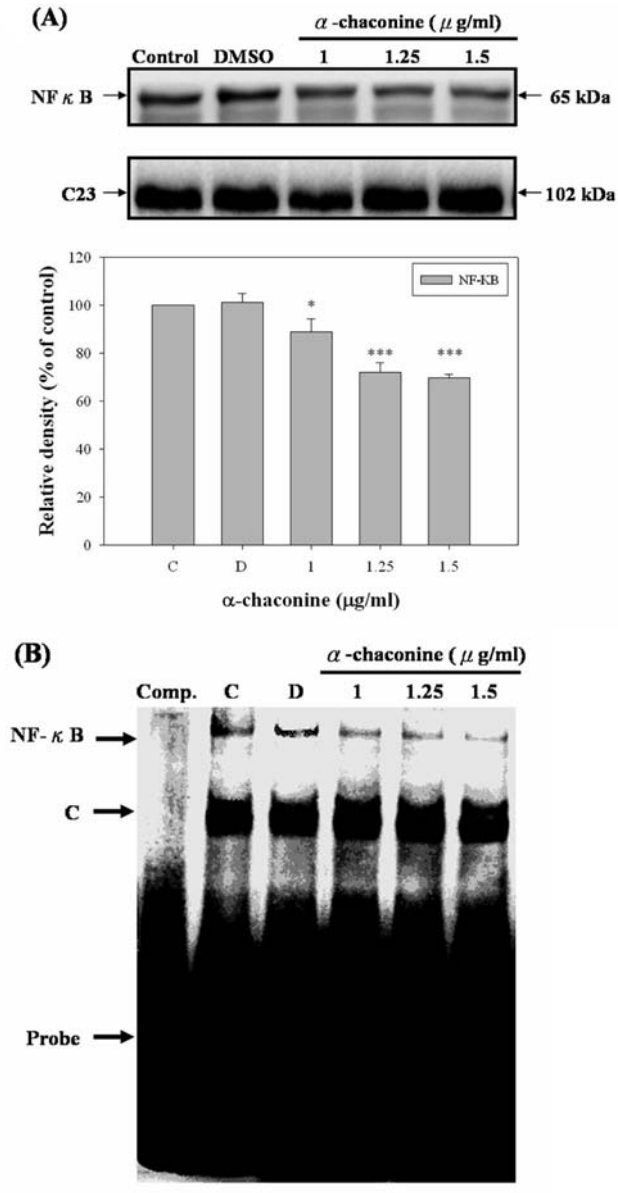

Figure 8. Effect of α-chaconine on the expression level of NF-κB and DNA binding activity of NF-κB. A549 cells were treated with or without α-chaconine; Control (C); 0.2% DMSO (D); 1, 1.25, and 1.5 μg/mL for 24 h. (**A**) Cell nuclear extracts were prepared and analyzed by Western blotting with anti-NF-κB (p65) antibody. C23 was a nucleus protein loading control. Determined activities of NF-κB were subsequently quantified by densitometric analysis with that of the control, which was 1.0 fold. The densitometric results are expressed as mean ± SD of three independent experiments. $^{*}p < 0.05$, $^{***}p < 0.001$ compared with the untreated control. (**B**) Cell nuclear extracts were prepared and analyzed for NF-κB DNA binding activity using biotin-labeled consensus NF-κB specific oligonucleotide, then the EMSA assay was performed as described in the Materials and Methods section. Lane 1: nuclear extracts incubated with a 100 fold excess of unlabeled consensus oligonucleotide (comp.) to confirm the specificity of binding. The position of NF-κB complex and free oligonucleotide were indicated. Results from three repeated and separated experiments were similar.

In conclusion, in the present study, we demonstrated that α-chaconine inhibits A549 cells, may be involved in the PI3K/Akt signaling pathway, exerts inhibitory effects on NF-κB transcriptional factor, and decreased DNA binding activity of NF-kB to NF-kB response element, which decreased MMP-2 and MMP-9 activities and then exerts an antimetastasis effect in the in vitro model. Taken together, these results indicated that either suppression of PI3K/Akt/NF-κB signals or the inhibition of MMP-2 and MMP-9 may be helpful in developing new chemotherapeutic strategies for A549 human lung adenocarcinoma cells.

LITERATURE CITED

(1) Jadhav, S. J.; Sharma, R. P.; Salunkhe, D. K. Naturally occurring toxic alkaloids in foods. *Crit. Rev. Toxicol.* **1981**, *9*, 21–104.

(2) Morris, S. C.; Lee, T. H. The toxicity and teratogenicity of *Solanaceae* glycoalkaloids, particularly those of the potato (*Solanum tuberosum*): a review. *Food Technol. Aust.* **1984**, *36*, 118–124.

(3) Cham, B. E.; Meares, H. M. Glycoalkaloids from *Solanum sodomaeum* are effective in the treatment of skin cancers in man. *Cancer Lett.* **1987**, *36*, 111–118.

(4) Kuo, K. W.; Hsu, S. H.; Li, Y. P.; Lin, W. L.; Liu, L. F.; Chang, L. C.; Lin, C. C.; Lin, C. N.; Sheu, H. M. Anticancer activity evaluation of the solanum glycoalkaloid solamargine. Triggering apoptosis in human hepatoma cells. *Biochem. Pharmacol.* **2000**, *60*, 1865–1873.

(5) Hu, K.; Kobayashi, H.; Dong, A.; Jing, Y.; Iwasaki, S.; Yao, X. Antineoplastic agents. III: Steroidal glycosides from *Solanum nigrum*. *Planta Med.* **1999**, *65*, 35–38.

(6) Lee, K. R.; Kozukue, N.; Han, J. S.; Park, J. H.; Chang, E. Y.; Baek, E. J.; Chang, J. S.; Friedman, M. J. Glycoalkaloids and metabolites inhibit the growth of human colon (HT-29) and liver (HepG2) cancer cells. *J. Agric. Food Chem.* **2004**, *52*, 2832–2839.

(7) Greenlee, R. T.; Hill-Harmon, M. B.; Murray, T.; Thun, M. Cancer statistics. *CA Cancer J. Clin.* **2001**, *51*, 15–36.

(8) Shivapurkar, N.; Reddy, J.; Chaudhary, P. M.; Gazdar, A. F. Apoptosis and lung cancer, A review. *J. Cell. Biochem.* **2003**, *88*, 885–898.

(9) Lee, G. Y.; Jang, J. S.; Lee, S. Y.; Jeon, H. S.; Kim, K. M.; Choi, J. E.; Park, J. M.; Chae, M. H.; Lee, W. K.; Kam, S.; Kim, I. S.; Lee, J. T.; Jung, T. H.; Park, J. Y. XPC polymorphisms and lung cancer risk. *Int. J. Cancer* **2005**, *115*, 807–813.

(10) Shih, J. Y.; Tsai, M. F.; Chang, T. H.; Chang, Y. L.; Yuan, A.; Yu, C. J.; Lin, S. B.; Liou, G. Y.; Lee, M. L.; Chen, J. J.; Hong, T. M.; Yang, S. C.; Su, J. L.; Lee, Y. C.; Yang, P. C. Tanscription repressor slug promotes carcinoma invasion and predicts outcome of patients with lung adenocarcinoma. *Clin. Cancer Res.* **2005**, *11*, 8070–8078.

(11) Bernhard, E. J.; Gruber, S. B.; Muschel, R. J. Direct evidence linking expression of matrix metalloproteinase 9 (92-kDa gelatinase/collagenase) to the metastatic phenotype in transformed rat embryo cells. *Proc. Natl. Acad. Sci. U.S.A.* **1994**, *91*, 4293–4297.

(12) Emmert-Buck, M. R.; Roth, M. J.; Zhuang, Z.; Campo, E.; Rozhin, J.; Sloane, B. F.; Liotta, L. A.; Stetler-Stevenson, W. G. Increased gelatinase A (MMP-2) and cathepsin B activity in invasive tumor regions of human colon cancer samples. *Am. J. Pathol.* **1994**, *145*, 1285–1290.

(13) Herbst, R. S.; Yano, S.; Kuniyasu, H.; Khuri, F. R.; Bucana, C. D.; Guo, F.; Liu, D.; Kemp, B.; Lee, J. J.; Hong, W. K.; Fidler, I. J. Differential expression of E-cadherin and type IV collagenase genes predicts outcome in patients with stage I non-small cell lung carcinoma. *Clin. Cancer Res.* **2000**, *6*, 790–797.

(14) Chan-Hui, P. Y.; Weaver, R. Human mitogen-activated protein kinase kinase kinase mediates the stress-induced activation of mitogen-activated protein kinase cascades. *Biochem. J.* **1998**, *336*, 599–609.

(15) Westermarck, J.; Kahari, V. M. Regulation of matrix metalloproteinase expression in tumor invasion. *Faseb. J.* **1999**, *13*, 781–792.

(16) Liao, D. W.; Wang, L.; Zhang, X. G.; Liu, M. Q. Expression and significance of PTEN/PI3K signal transduction-related proteins in non-small cell lung cancer. *Ai. Zheng.* **2006**, *25*, 1238–1242.

(17) Mosmann, T. Rapid colorimetric assay for cellular growth and survival: application to proliferation and cytotoxicity assays. *J. Immunol. Methods* **1983**, *65*, 55–63.

(18) Ochi, Y.; Atsumi, S.; Aoyagi, T.; Umezawa, K. Inhibition of tumor cell invasion in the Boyden chamber assay by a mannosidase inhibitor, mannostatin A. *Anticancer Res.* **1993**, *13*, 1421–1424.

(19) Chu, S. C.; Chiou, H. L.; Chen, P. N.; Yang, S. F.; Hsieh, Y. S. Silibinin inhibits the invasion of human lung cancer cells via decreased productions of urokinase-plasminogen activator and matrix metalloproteinase-2. *Mol. Carcinog.* **2004**, *40*, 143–149.

(20) Hoppe-Seyler, F.; Butz, K.; Rittmuller, C.; von Knebel Doeberitz, M. A rapid microscale procedure for the simultaneous preparation of cytoplasmic RNA, nuclear DNA binding proteins and enzymatically active luciferase extracts. *Nucleic Acids Res.* **1991**, *19*, 5080.

(21) Ma, W.; Lim, W.; Gee, K.; Aucoin, S.; Nandan, D.; Kozlowski, M.; Diaz-Mitoma, F.; Kumar, A. The p38 mitogen-activated kinase pathway regulates the human interleukin-10 promoter via the activation of Sp1 transcription factor in lipopolysaccharide-stimulated human macrophages. *J. Biol. Chem.* **2001**, *276*, 13664–13674.

(22) Yang, S. A.; Paek, S. H.; Kozukue, N.; Lee, K. R.; Kim, J. A. α-Chaconine, a potato glycoalkaloid, induces apoptosis of HT-29 human colon cancer cells through caspase-3 activation and inhibition of ERK 1/2 phosphorylation. *Food Chem. Toxicol.* **2006**, *44*, 839–846.

(23) Murrer, D.; Breathnach, R.; Engelman, A.; Millon, R.; Bronner, G.; Flesch, H.; Dumont, P.; Eber, M.; Abecasis, J. Expression of collagenase related metalloproteinases genes in human lung or head and neck tumors. *Int. J. Cancer.* **1991**, *48*, 550–556.

(24) Kanayama, H.; Yokota, K.; Kurokawa, Y.; Murakami, Y.; Nishitani, M.; Kagawa, S. Prognostic values of matrix metalloproteinase-2 and tissue inhibitor of metallo- proteinase-2 expression in bladder cancer. *Cancer (Phila.)* **1998**, *82*, 1359–1363.

(25) Kleiner, D. E.; Stetler-Stevenson, W. G. Matrix metalloproteinases and metastasis. *Cancer Chemother Pharmacol* **1999**, *43*, S42–S51.

(26) Kim, D.; Kim, S.; Koh, H.; Yoon, S. O.; Chung, A. S.; Cho, K. S.; Chung, J. Akt/PKB promotes cancer cell invasion via increased motility and metallolprteinases production. *FASEB J.* **2001**, *15*, 1953–1962.

(27) Chen, P. N.; Hsieh, Y. S.; Chiou, H. L.; Chu, S. C. Silibinin inhibits cell invasion through inactivation of both PI3K-Akt and MAPK signaling pathways. *Chem. Biol. Interact.* **2005**, *156*, 141–150.

(28) Turner, N. A.; Aley, P. K.; Hall, K. T.; Warburton, P.; Galloway, S.; Midgley, L.; O'regan, D. J.; Wood, I. C.; Ball, S. G.; Porter, K. E. Simvastatin inhibits TNFalpha-induced invasion of human cardiac myofibroblasts via both MMP-9-dependent and -independent mechanisms. *J. Mol. Cell Cardio.* **2007**, *43*, 168–176.

(29) Arboleda, M. J.; Lyons, J. F.; Kabbinavar, F. F.; Bray, M. R.; Snow, B. E.; Ayala, R.; Danino, M.; Karlan, B. Y.; Slamon, D. J. Overexpression of AKT2/protein kinase Bβ leads to up-regulation of β1 integrins, increased invasion, and metastasis of human breast and ovarian cancer cells. *Cancer Res.* **2003**, *63*, 196–206.

(30) Vayalil, P. K.; Katiyar, S. K. Treatment of epigallocatechin-3-gallate inhibits matrix metalloproteinases-2 and -9 via inhibition of activation of mitogen-activated protein kinases, c-jun and NF-κB in human prostate carcinoma DU-145 cells. *Prostate* **2004**, *59*, 33–42.

(31) Hung, S. C.; Ho, C. T.; Lin-Shiau, S. Y.; Lin, J. K. Carnosol inhibits the invasion of B16/F10 mouse melanoma cells by suppressing metalloproteinase-9 through down-regulating nuclear factor-κB and c-Jun. *Biochem. Pharmacol.* **2005**, *69*, 221–232.

Received for review August 12, 2007. Revised manuscript received October 26, 2007. Accepted November 1, 2007. This work was supported by the grant from the National Science Council of Taiwan (NSC95-2321-B-040-001).

JF072423R